Na^+,K^+-Adenosine Triphosphatase Polarity in Retinal Photoreceptors: A Role for Cytoskeletal Attachments

Steven A. Madreperla,* Michael Edidin,‡ and Ruben Adler*

Wilmer Institute,*School of Medicine, and ‡Department of Biology, Johns Hopkins University, Baltimore, Maryland 21205

Abstract. We have used isolated embryonic photoreceptor cells as a model system with which to examine the mechanisms responsible for the development and maintenance of asymmetric Na^+,K^+-ATPase (ATPase) distribution. Photoreceptor precursors, which appear round and process free at culture onset, develop structural and molecular properties similar to those of photoreceptor cells in vivo. ATPase, recognized by an anti-ATPase antibody, is distributed over the entire surface of round photoreceptor precursors. As the cells develop, ATPase becomes progressively concentrated in the inner segment (where it is found in cells of the intact retina). This phenomenon occurs in cells developing in the absence of intercellular contacts. The development of ATPase polarity correlates with a decrease in the fraction of ATPase molecules that are mobile in the membrane (as determined by fluorescence photobleaching recovery), as well as with an increase in the fraction of ATPase that remains associated with the cells after detergent extraction. The magnitudes of the mobile ATPase fractions agree well with those of the detergent-extractable fractions in both the immature and developed photoreceptors. The distribution of α spectrin and ATPase-immunoreactive materials appeared qualitatively similar, and quantitative image analysis showed similar gradients of spectrin and Na^+,K^+-ATPase immunofluorescence along the long axis of elongated photoreceptors. Moreover, detergent extractability of α spectrin and the ATPase showed similar modifications in response to changes in pH or KCl concentration. ATPase detergent-extractable and mobile fractions were not changed in cultures treated with cytoskeletal inhibitors such as nocodazole. These data are consistent with a role for an asymmetrically distributed, spectrin-containing subcortical cytoskeleton in the preferential accumulation of Na^+,K^+-ATPase in the photoreceptor inner segment.

THE plasma membrane of most cells in tissues is organized into domains differing in morphology and molecular composition (Almers and Stirling, 1984). The capacity to generate such domains and to polarize cell surfaces is crucial to cells' function (e.g., Axelrod, 1983). However, little is known about how domains are established during cell differentiation.

The retinal photoreceptor is organized into a series of domains that have different functions and distinct plasma membrane constituents. The outer segment, where phototransduction begins, is rich in the visual pigment opsin (Bok, 1985; Besharse, 1986; Papermaster et al., 1986), whereas the adjacent inner segment, which participates in generating the dark current, is poor in opsin but contains a high concentration of Na^+, K^+-ATPase (henceforth referred to as "ATPase") (Stirling and Lee, 1980; Ueno et al., 1984; Stahl and Baskin, 1984; Stirling and Sarthy, 1985; Yazulla and Studholme, 1987; Spencer et al., 1988).

Development of photoreceptor membrane polarity can now be studied in cultures of dissociated retinal cells. Recent studies have shown that chick embryo photoreceptors, grown in the absence of intercellular contacts, develop and maintain polarized properties that include asymmetries in both cell structure and distribution of molecules (Adler et al., 1984; Adler, 1986; Madreperla and Adler, 1989). We now report that the Na^+, K^+-ATPase of these cells is asymmetrically distributed, concentrated in the plasma membrane of the inner segment region, resembling the distribution in vivo. Analyses of the cultured cells using anticytoskeletal drugs, immunocytochemistry, detergent extraction, image analysis, and fluorescence photobleaching recovery (FPR)[1] are consistent with a role for a polarized, spectrin-containing cytoskeleton in photoreceptor ATPase polarity. The development of ATPase polarity in isolated photoreceptors, grown in the absence of intercellular contacts, is consistent with previous studies suggesting that intracellular cytoskeletal mechanisms are important determinants of autonomously generated photoreceptor asymmetries (Madreperla and Adler, 1989).

Address correspondence to Dr. Ruben Adler, 519 Maumenee Bldg., Johns Hopkins Hospital, 600 N. Wolfe St., Baltimore, MD 21205.

1. *Abbreviations used in this paper*: FPR, fluorescence photobleaching and recovery; TX-100, Triton X-100.

Materials and Methods

Materials

Medium 199, linoleic acid-BSA, polyornithine, paraformaldehyde, trypsin, Triton X-100, Pipes, Hepes, EGTA, polyethylene glycol (molecular weight 15,000–20,000), cytochalasin D, nocodazole, protein A-Sepharose and Sephadex G-100, G-25 were obtained from Sigma Chemical Co. (St. Louis, MO). Glass coverslips with grids were purchased from Belco (Vineland, NJ). Rhodamine- and fluorescein-conjugated goat anti-rabbit secondary antibodies were purchased from Jackson Immunoresearch Laboratories (Westgrove, PA). Gelvatol was obtained from Monsanto Corp. (Springfield, MA).

Cell Culture Preparation

The cell culture techniques used have been previously described in detail (Adler et al., 1984; Adler, 1986). Briefly, retinal cells were obtained from 8-d white Leghorn chick embryos. Neural retinas, free of contamination from pigment epithelial cells or other cells, were dissociated after brief trypsinization and suspended in medium 199 and supplemented with FCS (10%) and linoleic acid-BSA (110 μg/ml). 2-ml aliquots containing 400,000 cells/ml were seeded into 35-mm dishes that usually contained a glass coverslip. In all cases, dishes and coverslips were pretreated with polyornithine (50 μg/ml). The cultures were incubated at 37°C in an atmosphere of 5% CO_2 in air.

Cytochemistry

Cultured cells were prepared for immunocytochemistry by fixation in 4% paraformaldehyde for 30 min, followed in some cases by 10 min treatment with 0.25% Triton X-100 to permeabilize the cells. The AX-2 (formerly A-2) antiserum of McGrail and Sweadner (1986) was used for Na^+, K^+-ATPase immunocytochemistry in most cases. However, at later stages of this work, a rabbit antiserum raised against bovine brain ATPase became available to us (Siegel et al., 1988) and it was used for studies of cell surface immunoreactivity in nonpermeabilized cells (Fig. 6). Moreover, fluorescein-labeled Fab fragments of this antibody were used for fluorescence photobleaching and recovery studies (see below). For α spectrin immunocytochemistry, we used the antiserum of Glenney et al. (1982). Primary antisera were diluted between 1:150 and 1:250 and added to cells on coverslips in a humidified chamber for 1 h at room temperature. After washing three times for 5 min each in PBS, a rhodamine-conjugated secondary antiserum (1:40) was added for 40 min at room temperature. Cultures were washed again and mounted under a coverslip with Gelvatol. Control experiments included omission of primary antisera or use of nonimmune sera. These control preparations showed diffuse, low-level immunofluorescence (data not shown), very different from the specific patterns of immunostaining seen with the spectrin and ATPase antisera (e.g., Fig. 1).

Detergent Extraction Experiments

Cells in cultures were detergent extracted using a procedure similar to that of McOsker and Bretscher (1985). Unfixed cultures were incubated at 37°C for 4 min in a buffer containing 100 mM Pipes, pH 6.9, 2 mM EGTA, 4% polyethyleneglycol (molecular weight 15,000-20,000) (buffer S) and 0.2% to 0.4% Triton X-100 (TX-100). The buffer was removed and cells were fixed immediately in buffer S + 4% paraformaldehyde for 45 min at room temperature. Cells were washed several times in PBS and processed for immunocytochemistry as detailed above. The maximum detergent concentration that gave consistent fluorescence intensity measurements from cell to cell, and which preserved overall photoreceptor morphology was 0.4% TX-100. At higher detergent concentrations (e.g., 0.5% TX-100) fluorescence intensity measurements became very variable (>50% difference between cells) and photoreceptor morphology was markedly distorted.

Experiments with Anticytoskeletal Drugs

These experiments were performed as described previously (Madreperla and Adler, 1989). Cytochalasin D and nocodazole were prepared as 200× stocks in DMSO and added to cultures to reach final concentrations of 5 μM for cytochalasin D or 10 μM for nocodazole. After either 1.5 (cytochalasin D) or 4 h (nocodazole), some cultures were fixed in 4% paraformaldehyde, while others received three 5-min washes with 2 ml of inhibitor-free, fresh medium at 37°C, and were allowed to recover for up to 8 h before fixation. For fluorescence photobleaching and recovery studies (see below), cultures were treated with cytochalasin D or nocodazole for 1.5 or 4 h, respectively, and then labeled with Fab fragments.

Fluorescence Quantification by Image Analysis

Cultures immunostained using rhodamine-conjugated secondary antibodies were observed using a microscope (Diaphot; Nikon, Inc., Garden City, NY) with epifluorescence illumination (excitation at 540 nm with 15 nm bandpass), using a 100X oil immersion lens (na = 1.25). The small depth of focus of this objective allowed focusing on the cell surface. Background fluorescence/camera dark current was subtracted from each cell image before analysis. Images collected with an image intensifier (Videoscope Inc., Washington, DC) combined with a television camera (CCD; Sony Corp., Long Island City, NY) were digitized and analyzed with a digital image analysis system (IC200; Inovision Inc., Research Triangle Park, NC) running on a Sun 3/110 workstation (Sun Microsystems, Inc., Mountain View, CA). Average pixel intensity within a defined rectangular area (typically 500–3,600 pixels, or ~20 μm^2) was determined from the corrected image.

Measurements of ATPase Mobility by FPR

The mobility of Na^+,K^+-ATPase in the plane of the photoreceptor plasma membrane was measured by spot photobleaching of cells labeled with fluorescent Fab fragments of IgG from a rabbit antiserum against bovine brain ATPase (Siegel et al., 1988). Previous studies have shown that mobility of membrane proteins was the same with probes attached to their internal domain or with Fab fragments attached to their external domain, suggesting that Fab attachment did not alter membrane protein mobility (Packard et al., 1986). The Fab fragments were prepared by standard papain digestion (Porter, 1959). The digest was refractionated on protein A-Sepharose to remove any undigested IgG and then by size on Sephadex G100. The peak of Fab fragments was conjugated with FITC (15 μg FITC/mg protein in 0.1 M carbonate/bicarbonate for 12 h at 5°C). Conjugated Fab was separated from excess fluorescein on a G-25 column equilibrated with PBS (pH 7.3), then dialyzed against Hepes-buffered saline, pH 7.3. Protein concentration of the conjugate was ~300 μg/ml with a fluorescein/protein ratio of 2:3. The signal generated by these FITC-labeled Fab fragments was too weak for immunofluorescence photography, but was adequate for FPR measurements. An important control showed that labeling was specific, in that it was blocked by an excess of unlabeled IgG. Fluorescence intensity values of unlabeled cells were 20–25% of those measured in Fab-labeled cells. Given that it is technically difficult to focus on the surface of unlabeled cells, these measurements are probably an overestimate of the autofluorescence, because one tends to focus within the cytoplasm.

Our photobleaching measurements were made on a computer-controlled instrument. The 488 nm line of 3.5 W argon laser (Coherent, Inc., Palo Alto, CA) was attenuated 5,000-fold and focused to a spot of ~1 μm^2 on the surface of a cultured photoreceptor labeled with fluorescent Fab anti-ATPase. After recording fluorescence from this spot, the laser intensity was raised to maximum for 5–10 ms, bleaching a fraction of the fluorescence in the spot. The attenuated laser beam was then used to monitor recovery of fluorescence in the bleached spot. The recovery curves yield two parameters, the maximal extent of recovery of fluorescence and a half-time for maximal recovery. The half-time is related to the diffusion coefficient of the label as 1/area of the bleached spot. The extent of recovery indicates the fraction or percentage of labeled molecules free to diffuse in the plane of the membrane. The extent of this recovery may be reduced if a significant fraction of all the molecules in a membrane are bleached, the case for relatively large spots on small cells. We used a 40× na-1.3 oil immersion objective and an auxillary lens to define a spot of ~1.1 μm^2. This is insignificant compared with the labeled surface of a typical photoreceptor cell (~200 μm^2).

Results

Na^+,K^+-ATPase and Spectrin are Codistributed in Elongated Photoreceptor Cells In Vitro

Photoreceptors in vivo are divided into compartments, including an outer segment, an inner segment, a nucleus, and an axon with a complex synaptic ending.[2] Chicken cone

2. "Apical" is used to indicate the inner segment end of photoreceptors, while basal refers to the opposite, neurite-containing pole. "Above" and "below" are used to refer to structures located toward the apical or basal end of the cell, respectively.

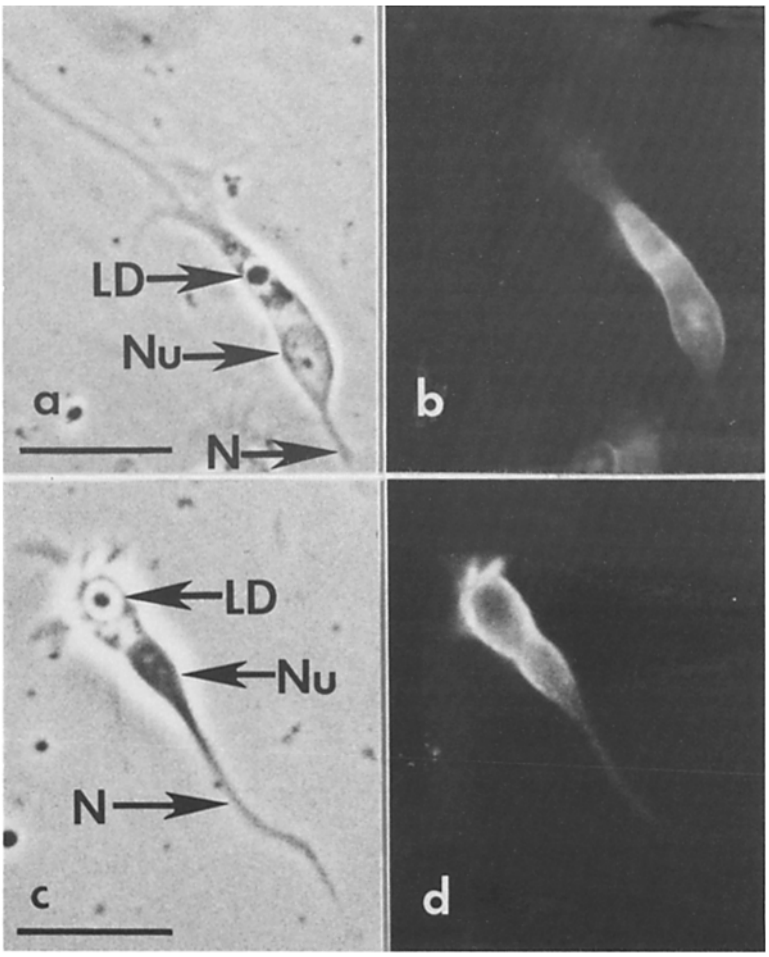

Figure 1. Na^+,K^+-ATPase and spectrin immunoreactivity in photoreceptors cultured for 6 d. (*a* and *b*) Cell immunoreacted with an antiserum against ATPase; (*c* and *d*) cell immunoreacted with an antiserum against spectrin (see text). (*a* and *c*) Phase-contrast microscopy. (*b* and *d*) immunofluorescence. Photoreceptors appear highly polarized, and are subdivided in compartments including the short neurite (*N*), the cell body, occupied by the nucleus (*Nu*), and the inner segment with a conspicuous lipid droplet (*LD*). A small outer segment can be seen by electron microscopy, but is not obvious in phase-contrast photomicrographs. Both ATPase and spectrin immunoreactive materials are concentrated in the inner segment region as well as over the apical[2] portion of the nuclear compartment. A variable amount of membranous-appearing material is present above the inner segment region of these cells which does not show immunoreactivity for either the ATPase or spectrin. Bar, 15 μm.

photoreceptors grown in vitro develop a very similar set of cellular compartments (Adler, 1986; see also Fig. 1 *a*). Convenient and reliable visual landmarks are the inner-segment lipid droplet (for the apical region of the cell) and the point at which the short neurite emerges from the cell body (for the opposite, or basal end). In vitro, the apical end of the cell also shows a membranous expansion (e.g., Fig. 1 *b*) and a small outer segment–like process (not seen) that usually appears in a different focal plane than the rest of the cell (Adler et al., 1984). Opsin immunoreactive materials accumulate in this outer segment–like process (Adler, 1986). Cultured photoreceptors develop and maintain this polarized pattern of organization even when grown in the absence of contacts with other cells.

Immunocytochemical Analysis

ATPase could be detected in cultured photoreceptors using the AX-2 (formerly A-2) antiserum of McGrail and Sweadner (1986) (Fig. 1, *a* and *b*). Bright surface fluorescence was present in the inner segment and the apical portion of the nuclear compartment. Fluorescence intensity decreased towards the base of the cell and was at a minimum in the neurite. Immunocytochemistry also showed that the distribution of α-spectrin immunoreactivity was very similar to that of the ATPase (Fig. 1, *c* and *d*). Bright surface staining was concentrated in the inner segment and in the apical portion of the nuclear region. ATPase and spectrin colocalization was also observed in double-labeled preparations (not shown). The small outer segment–like process of the photoreceptors in vitro showed little spectrin immunoreactivity, consistent with in vivo immunocytochemical studies (Lazarides et al., 1984).

ATPase and Spectrin Immunoreactivity after Detergent Extraction

A cytoskeletal residue remains attached to the "substratum" (surface of the dish) after cultured cells are extracted with buffers containing non-ionic detergents (e.g., Ben Ze'ev et al., 1979). In addition, some membrane proteins are also resistant to detergent extraction, suggesting a role for interactions between transmembrane proteins and the cytoskeleton (e.g., Galvin et al., 1984; Jung et al., 1984; Richter-Landsberg et al., 1985; Rapraeger et al., 1986; Horst et al., 1987). When retinal cultures were extracted with a TX-100-containing buffer before fixation, both spectrin and ATPase could still be detected with antisera in the inner segment region of photoreceptors (Fig. 2).

The codistribution of spectrin and ATPase was further analyzed by performing detergent extractions under conditions previously shown to affect the subcortical cytoskeleton in erythrocytes (Bennett and Branton, 1977; Bennett and Stenbuck, 1980). Extraction in a buffer containing 0.2% TX-100 plus added KCl caused concentration-dependent decreases in the number of cells that remained immunoreactive

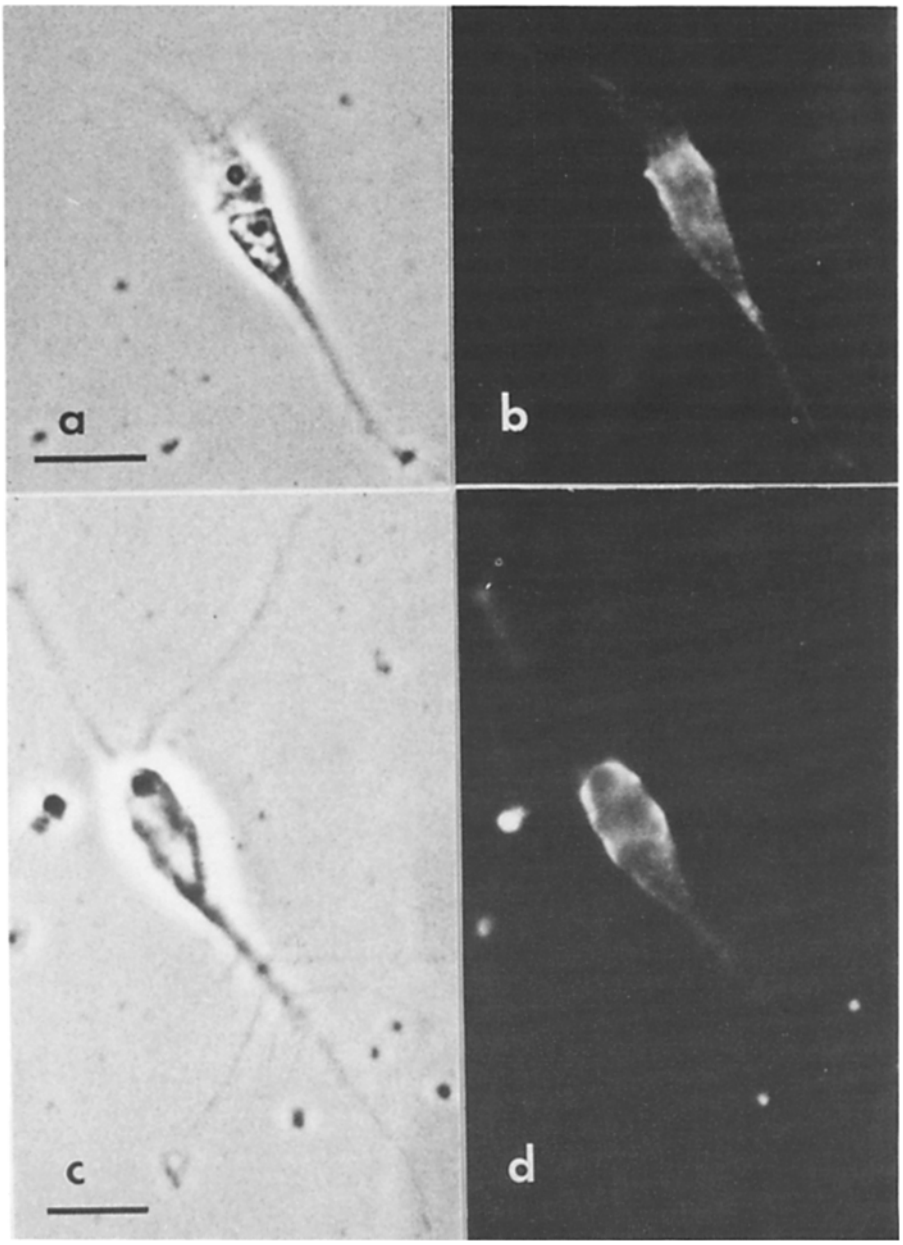

Figure 2. Na^+,K^+-ATPase (*b*) and spectrin immunoreactive materials (*d*) in photoreceptors cultured for 6 d and extracted for 4 min in 0.3% TX-100 before fixation. Corresponding phase-contrast images are shown in *a* and *c*. Surface staining is seen over the inner segment and part of the nuclear region of both cells. Bar, 10 μm.

for spectrin or ATPase (Fig. 3). The decreases were somewhat greater for ATPase than for spectrin at all the KCl concentrations tested. Analagous results were seen when detergent extractions were performed at pHs >7 or <6 (Fig. 3). Changes in frequency of antibody-labeled cells were similar for both antigens at most of the pHs studied. An exception was the presence of many fewer ATPase-positive cells than spectrin-positive cells in cultures extracted with detergent at pH 5. It is possible that resistance of spectrin to extraction at pH 5 was due to isoelectric aggregation occurring near the spectrin pKa (pKa = 4.8). Supporting this hypothesis were experiments that showed a twofold increase in the fraction of spectrin extracted at pH 5 when 0.5 M KCl was added.

Other cytoskeletal elements resisted extraction under conditions in which both ATPase and spectrin immunoreactivity were completely lost. For example, in cultures extracted at pH 4, actin filaments could still be demonstrated with rhodamine-phalloidin (not shown), and had a distribution similar to that previously reported for unextracted cells (Madreperla and Adler, 1989).

Analysis of digitized images of individual photoreceptors was also performed to quantify the levels of ATPase and spectrin immunofluorescence in cells extracted under several of the conditions described above (see Materials and Methods). The control values were the averages of fluorescence levels measured in cells detergent-extracted at pH 6.8 in the absence of added KCl. The average fluorescence levels in photoreceptors extracted at either pH 8 or pH 5 were expressed as a percentage of the average in control cells and showed decreases in both spectrin and ATPase immunofluorescence (Table I). Loss of ATPase label was somewhat greater than loss of spectrin at both pHs. Analogous results were seen in cultures extracted in the presence of 0.6M KCl.

Measurements of Spectrin and ATPase Gradients. Image

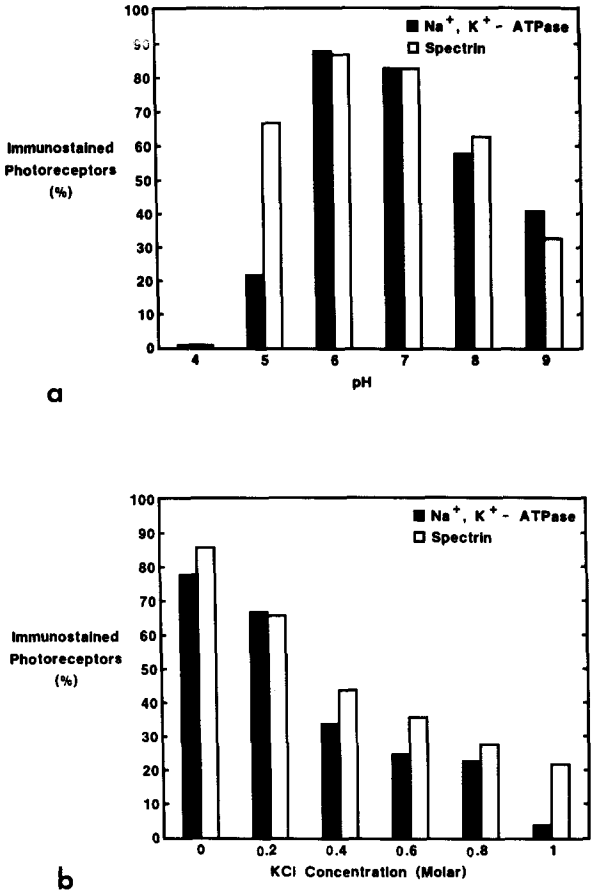

Figure 3. Histograms showing frequency of cells with positive immunostaining for Na^+,K^+-ATPase and spectrin after a 4-min extraction in 0.2% TX-100 at various pHs (*a*) and KCl concentrations (*b*). Approximately 50 cells were studied in each condition, and were scored as "positive" or "negative" by an observer who was unaware of the identity of each sample.

analysis was also used to compare the gradients of spectrin and ATPase immunofluorescence along the length of photoreceptors in 6-d-old cultures (Fig. 4). Relative fluorescence intensity is plotted versus the square of the distance from the position of maximum intensity in the inner segment, in cells immunostained for either spectrin or ATPase. The square of distance was used because the motion of a particle (diffusion) within a plane is a function of area (also see Discussion). ATPase and spectrin fluorescence intensities vary similarly, first dropping steeply and then gradually declining towards the basal end of the cells, eventually reaching 30–40% of the inner-segment maximum. This correlates with visual observations of high fluorescence in the inner segment, a steep drop over the nucleus, and further, gradual decrease towards the neurite (Fig. 1). As already indicated, no such gradients were observed in qualitative analyses of cells treated with nonimmune serum (data not shown).

Table I. Effects of pH and Ionic Strength on Extraction of Na^+,K^+-ATPase and Spectrin by Detergent

pH	KCl	Fluorescence remaining of control*	
		Na^+,K^+ATPase	Spectrin
	M	%	
5.0	0	29 ± 8.8	42 ± 7.9
8.0	0	46 ± 6.9	82 ± 17
6.8	0.6	23 ± 6.1	44 ± 15

* Detergent-extracted cultures were immunostained and the fluorescence intensity in the inner segment region of cells was measured by image analysis (see Materials and Methods). The average fluorescence intensity value was first determined for control cells that were detergent-extracted (see Materials and Methods) under normal conditions (pH 6.8, without added KCl) (n = 10). Next, the average fluorescence levels were determined for groups of cells (n = 10) in cultures that were detergent-extracted in buffers maintained at the pHs and KCl concentrations shown. The values given are the average fluorescence intensity values and the standard deviations (intraexperiment variability) for each experimental condition, divided by the average fluorescence intensity measured in the control cells expressed as percentages.

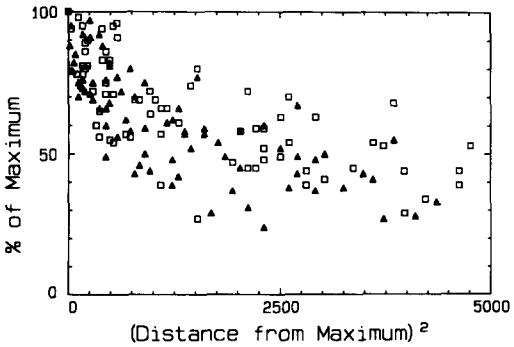

Figure 4. ATPase and spectrin immunofluorescence intensity gradient in elongated photoreceptors. Digitized images of immunofluorescent cells were obtained as described in Materials and Methods. A "mouse" was used to position points at the apical and basal ends of the video image of the photoreceptor cell body such that a line drawn between the two points bisected the cell body. Software gave the immunofluorescent intensity profile of the pixels along this line. The values were normalized to the maximum fluorescence value. The position of maximum fluorescence was defined as zero (this position always occurred in the inner segment) and relative intensity values were plotted versus the square of the distance (in pixels) from the position of maximum fluorescence. Distance was expressed in pixels units to avoid using a conversion factor. Data are shown for 30 cells. *Open boxes*, ATPase; *filled triangles*, spectrin.

Effects of Anticytoskeletal Drugs on ATPase Distribution

Cytochalasin D. As recently reported (Madreperla and Adler, 1989) depolymerization of actin filaments by cytochalasin D causes elongation of the photoreceptor cell body in vitro, with the nucleus moving away from the inner segment (Fig. 5, *a* and *b*). We have now observed that this treatment causes little change in ATPase distribution. ATPase immunoreactive materials remain associated with the inner segment and the apical portion of the nuclear compartment. Very little fluorescence is seen in the thin neck-like region that forms between the inner segment and nucleus (Fig. 5). The distribution of ATPase in cytochalasin D-treated cells that were returned to drug-free medium was similar to that in untreated cells (data not shown).

Nocodazole Treatments. It has been shown that loss of microtubules after nocodazole treatment causes the photoreceptor cell body to shorten, with the nucleus moving toward the inner segment and the cells eventually reverting to a round configuration after prolonged treatment (Madreperla and Adler, 1989). Fig. 5 *d* and *e* illustrates this phenomenon

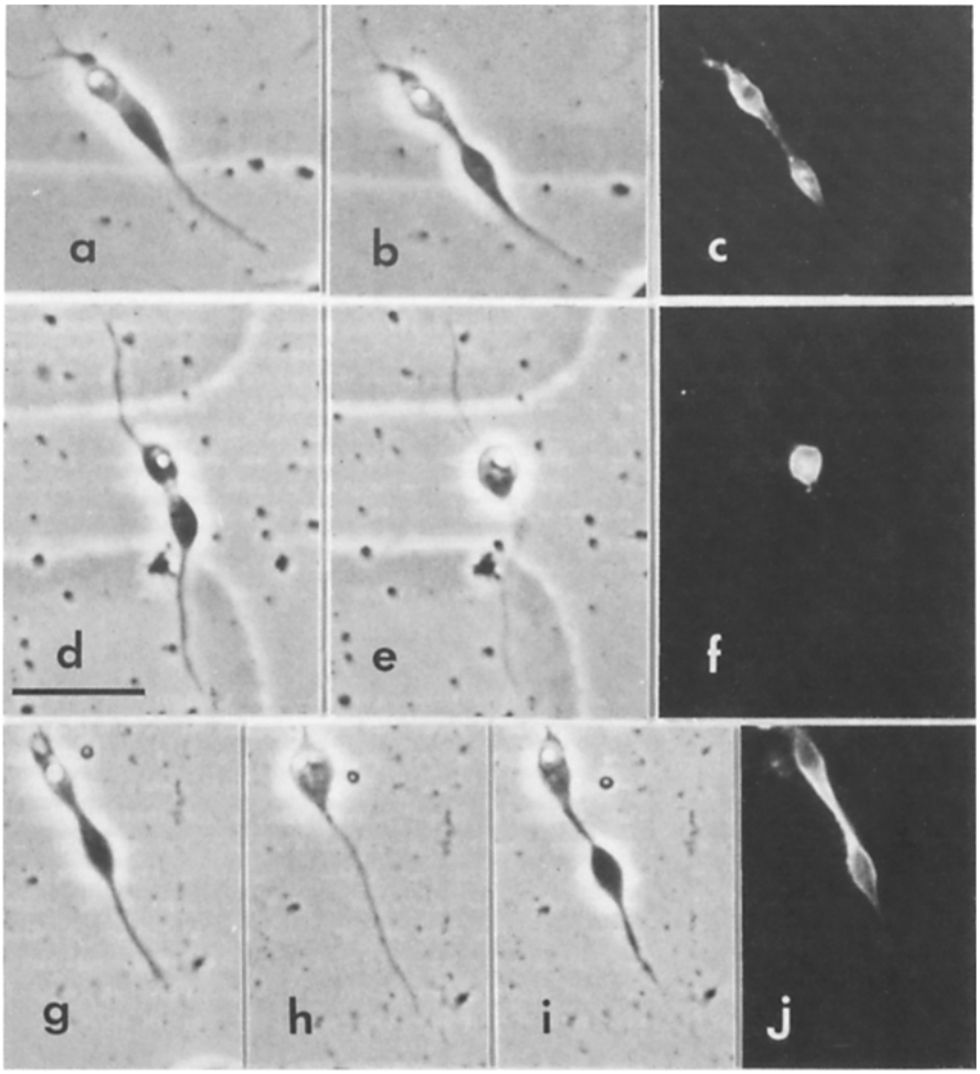

Figure 5. Effects of cytochalasin D (*a–c*) or nocodazole (*d–j*) treatment on shape and ATPase distribution in 5-d-old photoreceptors. A photoreceptor seen before (*a*) and 1.5 h after addition of 5 μM CCD. (*b*) Shows cell body elongation in response to the treatment, as the nucleus moves away from the inner segment (note positions relative to grid markers). When this cell was fixed and immunostained for ATPase (*c*), fluorescent materials could be seen in the inner segment and apical part of the nuclear region, but were not detectable in the thin "neck" that separates them. Another photoreceptor is shown before (*d*) and 4 h after addition of 10 μM nocodazole (*e*). As previously described, the cell body shortens to a round configuration in response to this treatment. When the same cell was fixed and immunostained for ATPase (*f*), fluorescence appeared diffusely distributed over the rounded cell body. Reversibility of this phenomenon is illustrated in *g–j*. A photoreceptor that collapses from an elongated (*g*) to a round configuration 4 h after addition of 10 μM nocodazole (*h*), can recover its elongated phenotype 8 h after being returned to fresh, nocodazole-free medium (*i*). ATPase immunocytochemistry (*j*) shows that the distribution of immunoreactive materials in this cell is restricted to the inner segment region and the apical portion of the nucleus, resembling the pattern seen in untreated cells (Fig. 1). Bar, 15 μm.

in a cell exposed to 10 μM nocodazole for 4 h. As seen in Fig. 5 *f*, ATPase immunoreactivity appeared symmetrically distributed around the circumference of nocodazole-treated cells. The nocodazole-treated cultures were returned to nocodazole-free medium to allow photoreceptors to regain their original elongated, compartmentalized configuration (Fig. 5, *h* and *i*). Immunocytochemistry showed that these cells reestablished a N^+,K^+-ATPase distribution similar to that seen in untreated cells (Fig. 5 *j*).

Quantitative measurement of the immunofluorescence remaining after detergent extraction was used to determine whether the association between the ATPase and the cytoskeleton was affected by nocodazole treatment. After extraction in 0.4% TX-100, no significant differences were observed in the amount of fluorescence remaining in nocodazole-treated compared with nocodazole-untreated cells. Fluorescence measurements were equal to 60.9 and 65% of the average level seen in unextracted cells, respectively (n = 10 cells in each group).

The Mobile Fraction of ATPase Molecules Correlates with Their Detergent Extractability

FPR Analysis. To further examine the apparent association with the cytoskeleton, ATPase lateral mobility was measured by FPR. Fluorescein-conjugated Fab fragments of an antibody raised against bovine brain ATPase (Siegel et al., 1987) were used to label photoreceptors in 6-d cultures. As shown in Fig. 6, this antibody recognized cell surface ATPase in unpermeabilized photoreceptors in culture. Fig. 7 *a* shows a typical photobleaching recovery curve obtained from a 6-d-old (differentiated) photoreceptor. The distribution of fractional recoveries measured in a series of 6-d-old photoreceptors is shown in Fig. 8 *a*. On average, 40% of the label was mobile in these cells (Table II), and the average diffusion coefficient of these mobile molecules was 2×10^{-9} cm^2s^{-1}. Correlating with the immunocytochemical and detergent extraction data described above, we found no significant changes in the mobile fractions of ATPase in cytochalasin D-treated

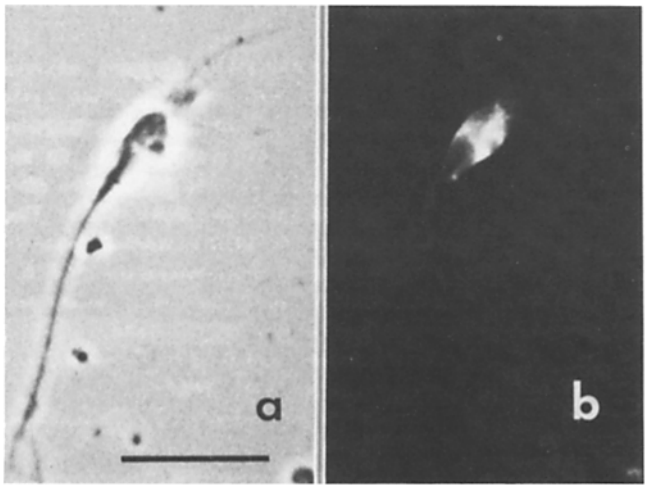

Figure 6. Na^+,K^+-ATPase immunocytochemistry in a fixed, nonpermeabilized cell. (*a*) phase contrast and (*b*) fluorescence of a 6-d-old cell fixed and immunostained without detergent treatment. Surface immunoreactive materials appear restricted to the inner segment region of the cell. Bar, 20 μm.

(mobile fraction = 32 ± 8%) or nocodazole-treated (mobile fraction = 37 ± 6%) photoreceptors. In control experiments, no fluorescence recovery was seen in cells fixed with 4% paraformaldehyde before FPR analysis (data not shown).

Detergent Extraction Experiments. Image analysis was used to quantify the fraction of ATPase involved in detergent-stable interactions with the cytoskeleton. In the 6-d-old photoreceptors with polarized ATPase, detergent extraction removed 41% of ATPase immunofluorescence (Table II). The magnitude of the detergent-extractable fraction is in good agreement with that of the mobile fraction determined by FPR.

ATPase and Spectrin in Developing Photoreceptors

Colocalization. As previously described (Madreperla and Adler, 1989, etc.), round photoreceptor precursors can be recognized after 24–30 h in culture by the presence of a lipid droplet. Their transformation into elongated cells involves a 12-h-long sequence of morphogenetic transformations that includes the extension of a neurite, followed by cell body elongation and the appearance of an apical membranous expansion. As shown in Fig. 9, both ATPase and spectrin immunoreactivities were uniformly distributed in some of the round precursor cells (Fig. 9, *a*, *f*, *k*, and *p*), but were concentrated near the lipid droplet in others (Fig. 9, *b*, *g*, *l*, and *q*). On the other hand, the latter pattern was always found in more developed, neurite-bearing round cells (Fig. 9, *c*, *h*, *m*, and *r*). As the cell body began to elongate (Fig. 9, *d*, *h*, *d*, and *n*), ATPase and spectrin immunoreactivities became more restricted to the developing inner segment region (Fig. 9, *i* and *s*). In cells that had developed further and extended a membranous expansion (Fig. 9, *e* and *o*), the polarized ATPase and spectrin patterns (Fig. 9, *j* and *t*) resembled very closely the distribution seen in fully elongated photoreceptors in 6-d cultures (e.g., Fig. 1).

Extractability and Mobility. A typical FPR curve for ATPase in a photoreceptor precursor cell is shown in Fig. 7 *b*, whereas Fig. 8 *b* shows the distribution of mobile fractions in a population of these cells. The average mobile fraction was 65%, more than one and one half times the value measured in elongated cells (40%, see above) with polarized ATPase staining (Table II). The difference in average recovery fractions between elongated and immature photoreceptors was statistically significant ($P < 0.001$). The average diffusion coefficient of the mobile molecules was 2.4×10^{-9} cm^2/s for the round precursors, not significantly different from that measured in the 6-d-old cells.

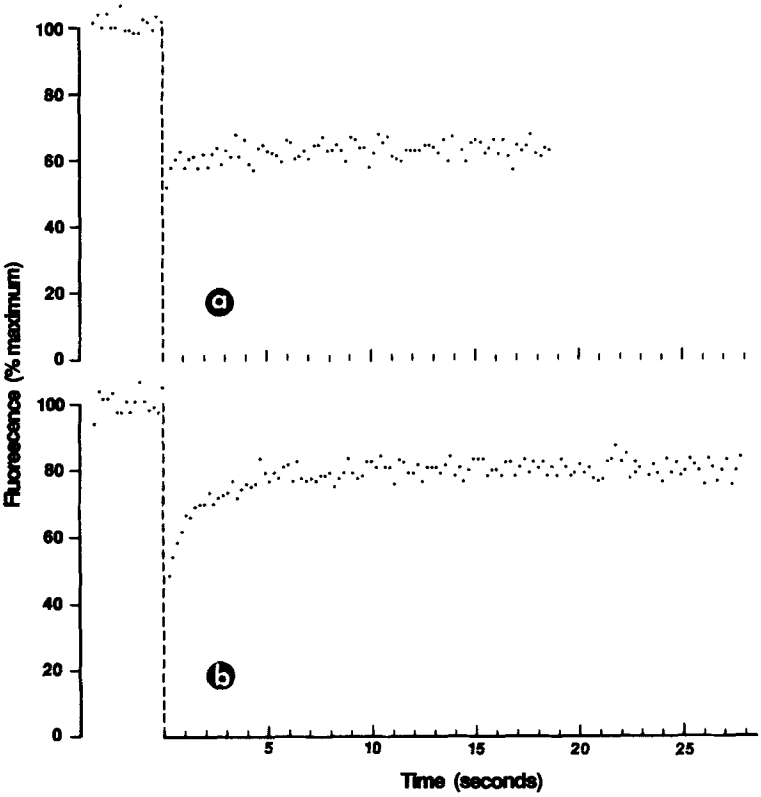

Figure 7. Typical fluorescence photobleaching recovery curves for (*a*) a mature, 6-d-old photoreceptor and (*b*) a round photoreceptor precursor in a 2-d-old culture. Cultures were labeled with FITC-conjugated Fab fragments of a Na^+,K^+-ATPase antiserum. Normalized fluorescence is plotted as a function of time. The vertical dashed line indicates time zero, when the photobleaching occurred. Although the visual perception may be different, the calculated $t_{1/2}$, to reach maximal fluorescence recovery (0.7 s) is the same in (*a*) and (*b*). The relationship between diffusion coefficient (D) and half-time is $D = (W^2/4t_{1/2})^{\Gamma}$, where W is the radius of the laser spot, and Γ is a factor dependent upon the extent of bleach (Γ varied between 1.1 and 1.4 in our experiments).

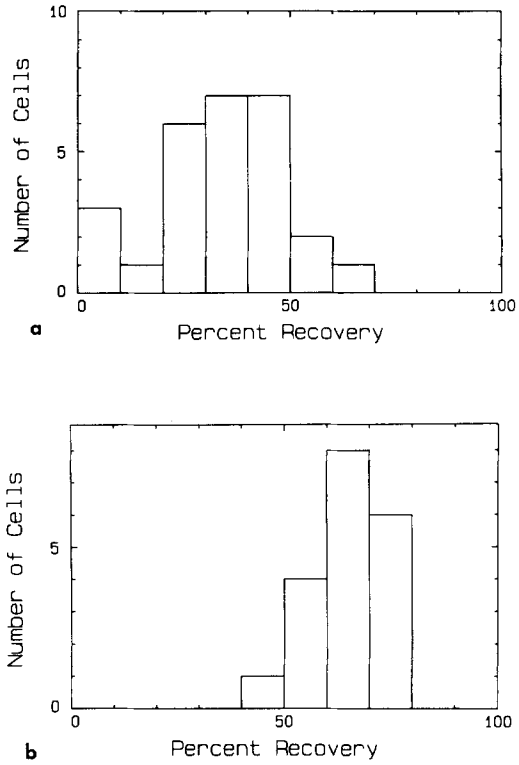

Figure 8. Distribution of FPR in (*a*) mature, 6-d-old photoreceptors and (*b*) round, photoreceptor precursors in 2-d-old cultures. Cultures were labeled with FITC-conjugated Fab fragments of a Na^+,K^+-ATPase antiserum. Fluorescence recovery was divided into 10 equal bins from 0 to 100%, and the histogram shows the numbers of cells with mobile fractions within each bin.

Round precursor cells were extracted with TX-100 and the remaining immunodetectable ATPase was quantified by image analysis. Table II shows that on average, 62% of the ATPase was extracted by detergent in immature, precursor cells, agreeing well with the average fractional recovery measured by FPR in these cells. The difference in ATPase detergent extractability between precursors and elongated cells was also statistically significant ($P < 0.001$).

Table II. Developmental Changes in Mobile and Detergent-extractable Fractions of Na^+,K^+-ATPase Molecules

	Mobile fraction		Detergent extractable	
	%	*n*	%	*n*
Round photoreceptor precursors	65 ± 11	19	62 ± 6.8	10
Elongated polarized photoreceptors	40 ± 9.0	28	41 ± 12	10

Mobile fractions were determined by FRP as described in Materials and Methods. The numbers of cells measured are shown as well as the SDs of the mean mobile fractions. To determine detergent extractability in cultures from both developmental stages, the average fluorescence intensity value was first determined for control cultures that were not detergent extracted ($n = 10$ at each developmental stage). Next, the average fluorescence levels were determined for groups of cells ($n = 10$) in cultures at both developmental stages, that were detergent extracted in 0.4% TX-100 (see Materials and Methods). The values given are the average fluorescence intensity values and the SDs (intraexperiment variability) for both developmental stages, divided by the average fluorescence intensity measured in the control cells at each stage. The differences in mobile fractions and in detergent-extractable fractions between precursors (round) and mature (elongated) photoreceptors were both significant ($P < 0.001$, *t* test).

Discussion

Using an experimental system that allows dynamic analysis of the behavior of identified embryonic precursor cells, grown in the absence of intercellular contacts, this laboratory recently reported that the cytoskeleton is important in the development and maintenance of structural polarity by photoreceptors (Adler, 1986; Madreperla and Adler, 1989). This type of analysis has now been extended to surface polarity, epitomized by the distribution of immunoreactive Na^+,K^+-ATPase, which in adult photoreceptors in vivo, is found predominantly concentrated in the inner segment plasma membrane (Ueno et al., 1984; Stahl and Baskin, 1984; Yazulla and Studholme, 1987; Spencer et al., 1988).

Our data show that isolated, cell contact-free photoreceptor precursors can develop and maintain a polarized pattern of ATPase distribution. Accumulation of ATPase immunoreactive materials in the inner segment region of elongated photoreceptors was determined by qualitative observations, and confirmed by quantitative image analysis of fluorescence intensities along the longitudinal axis of these cells. The variations in fluorescence intensity measured across the photoreceptor surface are unlikely to reflect differences in membrane density, because previous scanning electron microscopic studies have shown that cultured photoreceptors have a fairly smooth surface without microvilli or apparent membrane redundancy (Adler et al., 1984). ATPase polarity seems to be part of a complex developmental program to which photoreceptor precursor cells are already committed at the time of their isolation from the retina on embryonic day 8 (Adler, 1986; Madreperla and Adler, 1989; Adler and Hatlee, 1989).

Translational diffusion of membrane molecules will randomize cell membranes with time. Given that the surface areas of cells are small (hundreds of squared microns) and that the cells' lifetimes are long enough (days), even diffusion as small as 10^{-13} $cm^2 \cdot s^{-1}$ (smaller than has ever been measured for membrane proteins) would randomize surfaces. Hence, development of membrane protein domains must involve mechanisms working against lateral diffusion (Wolf, 1987). Some mechanisms that have been proposed include (*a*) barriers, such as tight junctions, that act as gates or fences; (*b*) specific removal of proteins from other membrane surfaces; and (*c*) restriction of surface protein mobility by local attachments to the cytoskeleton or to extracellular matrices (e.g., Axelrod, 1983; Almers and Stirling, 1984; Jesaitis and Yguerabide, 1986; Wolf, 1987). Of these possibilities, our data are most consistent with attachment of ATPase to a submembranous cytoskeleton. At the two stages of photoreceptor development examined in vitro, the magnitude of the average ATPase mobile fraction determined by FPR was similar to the average detergent-extractable fraction of ATPase determined by quantitative image analysis. Similar results were obtained in a previous study using other cells (Salas et al., 1988). The correlation between the mobile fractions and the detergent extractable fractions suggests that restriction of ATPase mobility is due to interaction with the cytoskeleton. Other workers have shown interactions between asymmetrically distributed membrane proteins (including Na^+,K^+-ATPase) and the cytoskeleton (e.g., Nelson and Veshnock, 1986; Rapraeger et al., 1986; Horst et al., 1987; Ojakian and Schwimmer, 1988). Experiments that

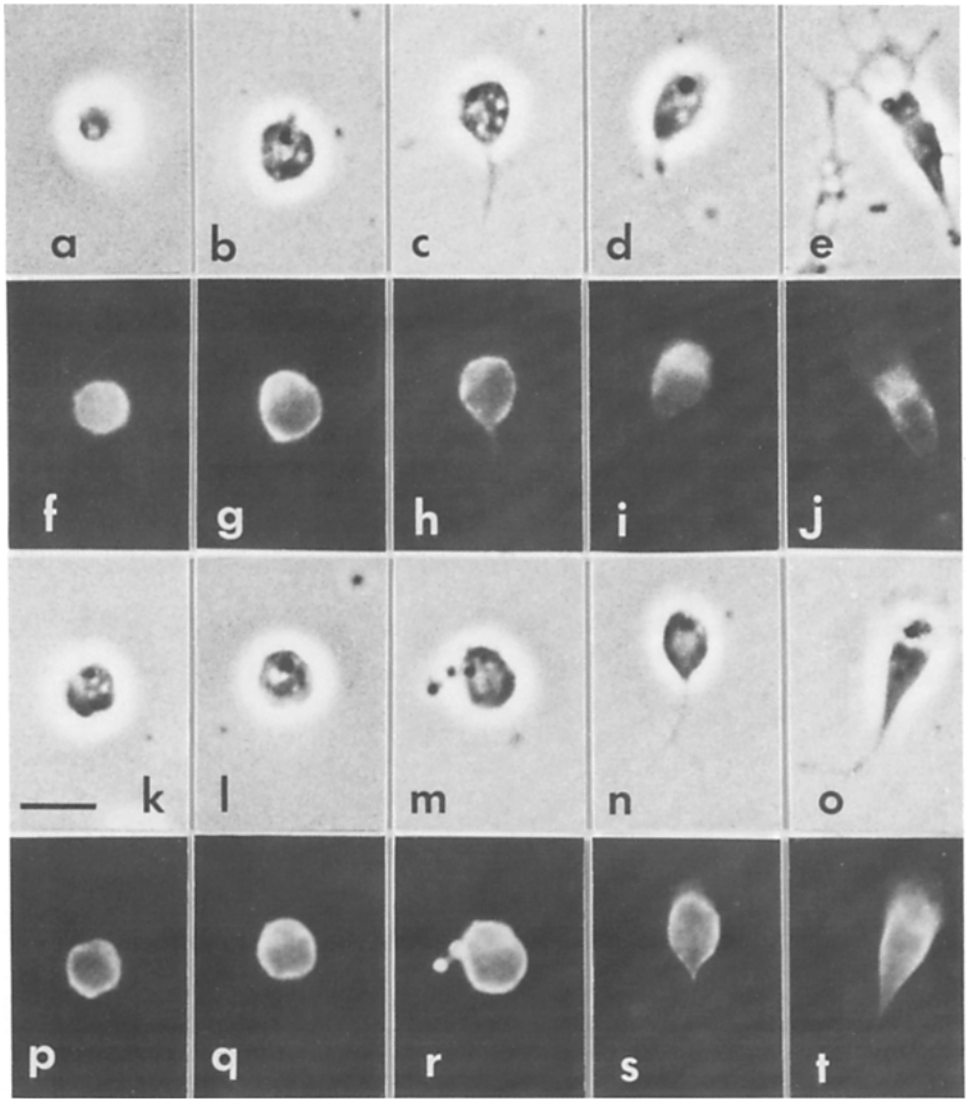

Figure 9. Developmental series showing ATPase and spectrin immunofluorescence in photoreceptors at various stages of morphogenesis, including round photoreceptor precursors (*a*, *b*, *f*, *g*, *k*, *l*, *p*, and *q*), round cells with a short neurite (*c*, *h*, *m*, and *r*), cells with elongated body (*d*, *i*, *n*, and *s*) and elongated cell with an apical membranous expansion (*e*, *j*, *o*, and *t*). *a–e* and *k–o* are phase-contrast micrographs; *f–j* and *p–t* show ATPase and spectrin immunofluorescence, respectively. Staining patterns for the ATPase and for spectrin are similar at each stage. Round photoreceptor precursors have a symmetric staining pattern in some cells (*f* and *p*) and an accumulation near the lipid droplet in others (*g* and *q*). This accumulation was always seen in round cells with a neurite (*h* and *r*). Elongated cells (*i* and *s*) begin to show extensive polarization of both antigens with the basal portion of the cells only having background level staining. (*j* and *t*) Elongated cells with a membranous expansion show patterns of immunoreactivity similar to those in mature cells, with immunoreactive materials concentrated in the developing inner segment region. Bar, 7.5 μm.

showed no change in Na^+, K^+-ATPase distribution after fusion of photoreceptor inner and outer segments suggested that ATPase interacts with the cytoskeleton in photoreceptors (Spencer et al., 1988).

A conclusion different than ours was reached by other authors who observed a greater Na^+,K^+-ATPase mobility in cultured MDCK cells and therefore proposed that the cytoskeleton was probably not critically involved in ATPase polarity in those cells (Jesaitis and Yguerabide, 1986). These different results could reflect differences between photoreceptors and epithelial cells and/or differences in the conditions used for FPR measurements, since the basolateral distribution of ATPase in cultured MDCK cells made it necessary to detach cells from the substratum before FPR analysis.

The gradients of ATPase and spectrin measured by image analysis were very similar. Throughout photoreceptor morphogenesis in vitro, the ATPase colocalized with spectrin. Variations in pH and salt concentration during exposure to detergents resulted in parallel changes in ATPase and spectrin extraction, although the amount extracted was always larger for ATPase than for spectrin. These data are suggestive of an interaction between spectrin and the ATPase. Other investigators have provided evidence of a direct linkage between the Na^+,K^+-ATPase and cytoskeletal proteins (Nelson and Veshnock, 1987; Koob et al., 1988; Morrow, 1989). Similar biochemical studies were not carried out with our preparations because of the heterogeneity of the retinal cultures, which contain neurons and undifferentiated cells in addition to the photoreceptors.

Results showing somewhat greater extraction of ATPase compared with spectrin are consistent with our finding of a fraction of mobile surface ATPase molecules even in differentiated, polarized cells. In turn, this suggests that direct attachment to the cytoskeleton may not completely account for polarization of photoreceptor surfaces. We could measure a population of mobile, detergent-soluble, molecules even in cells with polarized ATPase. In erythrocytes, where the relative immobility of band 3 is thought to involve interactions with spectrin (Cherry, 1981), a portion of the band 3 is readily extractable by Triton X-100 (Branton et al., 1983). This has led to the suggestion that corralling of membrane

proteins without direct binding to the cytoskeleton may also be involved in restricting membrane protein mobility. We know nothing of the origin or fate of the mobile ATPase molecules. They could be a pool of molecules newly arrived at the surface, which must compete with existing surface molecules for spectrin binding sites. Alternatively, they may represent molecules destined to be removed from the cell surface. Although the measured gradient of ATPase has the shape expected from diffusion of molecules from a limited insertion region, it follows the gradient of spectrin, ruling against the possibility that mobile ATPase molecules simply diffuse from an insertion region (in the inner segment) to some sink at the opposite end of the cell. However, due to the low concentration of labeled ATPase at the basal end of the cell, we were unable to measure ATPase mobility in these regions, and so cannot say with certainty that the proportions of mobile and anchored ATPase molecules are the same in regions of high and low ATPase concentrations.

Our studies suggest that other cytoskeletal components, such as cytochalasin D-sensitive actin filaments or nocodozole-sensitive microtubules are not involved in the restriction of ATPase mobility. Thus, despite its obvious effects on cell body length, cytochalasin D did not appear to cause marked changes in ATPase distribution. On the other hand, ATPase did become more uniformly distributed when nocodazole-treated photoreceptors lost their elongated shape and became rounded. However, this apparent loss of ATPase polarity was not associated with any detectable changes in ATPase extractability by detergent. Also, neither cytochalasin D nor nocodazole altered the fraction of mobile ATPase molecules. A relevant precedent for this observation is that no changes in lateral mobility of the voltage-sensitive Na^+ channel (also shown to interact with the subcortical cytoskeleton) were observed in colchicine-treated neurons (Angelides et al., 1988).

This paper has shown that isolated photoreceptor precursors can generate and maintain overlapping gradients of both spectrin and ATPase as they develop from a circular to an elongated pattern of morphological organization in the absence of intercellular contacts. Other neuronal cells also appear to be endowed with intracellular mechanisms capable of generating predictable shapes and of directing different molecular species to different cell regions in the absence of intercellular contacts (Dotti et al., 1988; Banker and Waxman, 1988; Garner et al., 1988; Goslin et al., 1988). Understanding the nature of the intracellular mechanisms through which these programs of development are implemented remains a challenging area for investigation.

We are most grateful to Dr. William Busa for the use of his image analysis system and invaluable help in designing experiments. We would like to thank Dr. Maribeth Spencer for some insightful discussions in the early part of this work. We also thank Drs. John Glenney, Kathleen Sweadner, and George Siegel for generous gifts of antisera. The authors are also indebted to Dr. M. Lehar, Mr. M. Hatlee, and Mrs. Taiyin Wei for technical assistance and to Mrs. Doris Golembieski for secretarial help.

This work was supported by U. S. Public Health Service grant EY-04859 to R. Adler and AI-4584 to M. Edidin. S. Madreperla is supported by National Institutes of Health Medical Scientist Training Program GM-07309.

Received for publication 24 January 1989 and in revised form 15 May 1989.

References

Adler, R. 1986. Developmental predetermination of the structural and molecular polarization of photoreceptor cells. *Dev. Biol.* 117:520–527.

Adler, R., and M. Hatlee. 1989. Plasticity and differentiation of embryonic retinal cells after terminal mitosis. *Science (Wash. DC).* 243:391–393.

Adler, R., J. D. Lindsey, and C. L. Elsner. 1984. Expression of cone-like properties by chick embryo neural retina cells in glial-free monolayer cultures. *J. Cell Biol.* 99:1173–1178.

Almers, W., and C. Stirling. 1984. Distribution of transport proteins over animal cell membranes. *J. Membr. Biol.* 77:169–186.

Angelides, K. J., L. W. Elmer, D. Loftus, and E. Elson. 1988. Distribution and lateral mobility of voltage-dependent sodium channels in neurons. *J. Cell Biol.* 106:1911–1925.

Axelrod, D. 1983. Lateral motion of membrane proteins and biological function. *J. Membr. Biol.* 75:1–10.

Banker, G. A., and A. B. Waxman. 1988. Hippocampal neurons generate natural shapes in cell culture. *In* Intrinsic Determinants of Neuronal Form and Function. R. J. Lasek and M. M. Black, editors. Alan R. Liss, Inc., New York. 61–82.

Ben-Ze'ev, A. Deurr, F. Solomon, and S. Penman. 1979. The outer boundary of the cytoskeleton: a lamina derived from plasma membrane proteins. *Cell.* 17:859–865.

Bennett, V., and D. Branton. 1977. Selective association of spectrin with the cytoplasmic surface of human erythrocyte plasma membranes. *J. Biol. Chem.* 252:2753–2763.

Bennett, V., and P. J. Stenbuck. 1980. Association between ankyrin and the cytoplasmic domain of band 3 isolated from the human erythrocyte membrane. *J. Biol. Chem.* 255:6424–6432.

Besharse, J. C. 1986. Photosensitive membrane turnover: differentiated domains and cell-cell interaction. *In* The Retina: A Model for Cell Biology Studies. Part I. R. Adler and D. Farber, editors. Academic Press, Orlando, FL. 297–339.

Bok, D. 1985. Retinal photoreceptor-pigment epithelial interactions. Friedenwald Lecture. *Invest. Ophthalmol. & Visual Sci.* 26:1659–1694.

Branton, D., Cohen, C. M., and J. Tyler. 1981. Interaction of cytoskeletal proteins on the human erythrocyte membrane. *Cell.* 24:24–32.

Cherry, R. J. 1981. Rotational diffusion of membrane proteins: measurements with bacteriorhodopsin, Band-3 proteins and erythrocyte oligosaccharides. *Biochem. Soc. Symp.* 46:183–190.

Dotti, C. G., C. A. Sullivan, and G. A. Banker. 1988. The establishment of polarity by hippocampal neurons in culture. *J. Neurosci.* 8:1454–1468.

Galvin, N. J., D. Stockhausen, B. L. Meyers-Hutchins, and W. A. Frazier. 1984. Association of the cyclic AMP chemotaxis receptor with the detergent-insoluble cytoskeleton of *Dictyostelium Discoideum. J. Cell Biol.* 98:584–595.

Garner, C. C., R. P. Tucker, and A. Matus. 1988. Selective localization of messenger RNA for cytoskeletal protein MAP-2 in dendrites. *Nature (Lond.).* 336:674–677.

Glenney, J. R., P. Glenney, and K. Weber. 1982. Erythroid spectrin, brain fodrin, and intestinal brush border proteins (TW-260/240) are related molecules containing a common calmodulin-binding subunit bound to a variant cell-type specific subunit. *Proc. Natl. Acad. Sci. USA.* 79:4002–4005.

Goslin, V., D. J. Schreyer, J. H. P. Skene, and G. Banker. 1988. Development of neuronal polarity: GAP-43 distinguishes axonal from dendritic growth cones. *Nature (Lond.).* 336:672–674.

Horst, C. J., D. M. Forestner, and J. C. Besharse. 1987. Cytoskeletal-membrane interactions: a stable interaction between cell surface glycoconjugates and doublet microtubules of the photoreceptor connecting cilium. *J. Cell Biol.* 105:2973–2987.

Jesaitis, A. J., and J. Yguerabide. 1986. The lateral mobility of the (Na^+,K^+)-dependent ATPase in Madin-Darby canine kidney cells. *J. Cell Biol.* 102:1256–1263.

Jung, G., R. M. Helm, C. A. Carothers-Carraway, and K. L. Carraway. 1984. Mechanism of concanavalin A-induced anchorage of the major cell surface glycoproteins to the submembrane cytoskeleton in 13762 ascites mammary adenocarcinoma cells. *J. Cell Biol.* 98:179–187.

Koob, R., M. Zimmerman, W. Schoner, and D. Drenckhahn. 1988. Colocalization and coprecipitation of ankyrin and Na^+,K^+-ATPase in kidney epithelial cells. *Eur. J. Cell Biol.* 45:230–237.

Lazarides, E., W. J. Nelson, and T. Kasamatsu. 1984. Segregation of two spectrin forms in the chicken optic system: a mechanism for establishing restricted membrane-cytoskeletal domains in neurons. *Cell.* 36:269–278.

Madreperla, S., and R. Adler. 1989. Opposing microtubule- and actin-dependent forces in the development and maintenance of structural polarity in retinal photoreceptors. *Dev. Biol.* 131:149–160.

McGrail, K. M., and K. J. Sweadner. 1986. Immunofluorescent localization of two different Na, K-ATPases in the rat retina and in identified dissociated retinal cells. *J. Neurosci.* 6:1272–1283.

McOsker, C. C., and A. Bretscher. 1985. Fodrin is part of a filamentous cortical sheath of the detergent resistant cytoskeleton of cultured cells before and after cytochalasin treatment. *Eur. J. Cell Biol.* 39:321–327.

Morrow, J. S., C. D. Cianci, T. Ardito, A. S. Mann, and M. K. Kashgarian. 1989. Ankyrin links fodrin to the alpha-subunit of Na^+,K^+-ATPase in Madin-Darby canine kidney and in intact renal tubule cells. *J. Cell Biol.* 108:455–465.

Nelson, W. J., and P. J. Veshnock. 1986. Dynamics of membrane-skeleton (fodrin) organization during development of polarity in Madin-Darby canine kidney epithelial cells. *J. Cell Biol.* 103:1751–1765.

Nelson, W. J., and P. J. Veshnock. 1987. Ankyrin binding to (Na^+ + K^+)ATPase and implications for the organization of membrane domains in polarized cells. *Nature (Lond.).* 328:533–536.

Ojakian, G. K., and R. Schwimmer. 1988. The polarized distribution of an apical cell surface glycoprotein is maintained by interactions with the cytoskeleton of Madin-Darby canine kidney cells. *J. Cell Biol.* 107:2377–2387.

Packard, B., I. Komriya, and M. Edidin. 1986. Biological and physical characterization of immunoglobulins fluorescently labeled across disulphide bonds. *Biophys. J.* 49:357*a*. (Abstr.)

Papermaster, D. S., B. G. Schneider, D. Defoe, and J. C. Besharse. 1986. Biosynthesis and vectorial transport of opsin on vesicles in retinal rod photoreceptors. *J. Histochem. Cytochem.* 34:5–16.

Porter, R. R. 1959. Hydrolysis of rabbit gamma-globulin and antibodies with crystaline papain. *Biochem. J.* 73:119–126.

Rapraeger, A., M. Jalkanen, and M. Bernfield. 1986. Cell surface proteoglycan associates with the cytoskeleton at the basolateral cell surface of mouse mammary epithelial cells. *J. Cell Biol.* 103:2683–2696.

Richter-Landsberg, C., L. A. Greene, and M. L. Shelanski. 1985. Cell surface Thy-1-cross-reactive glycoprotein in cultured PC12 cells: modulation by nerve growth factor and association with the cytoskeleton. *J. Neurosci.* 2:468–476.

Salas, P. J. I., D. E. Vega-Salas, J. Hochman, E. Rodriguez-Boulan, and M. Edidin. 1988. Selective anchoring in the specific membrane domain: a role in epithelial polarity. *J. Cell Biol.* 107:2363–2376.

Siegel, G. J., S. A. Ernst, J. L.-H. Liu, and T. J. Desmond. 1988. Heterogeneity of the α^+-catalytic subunit in mouse brain Na^+,K^+-ATPase. *Trans. Am. Soc. Neurochem.* 19:252.

Spencer, M., P. B. Detwiler, and A. H. Bunt-Milam. 1988. Distribution of membrane proteins in mechanically dissociated retinal rods. *Invest. Ophthamol. & Visual Sci.* 29:1012–1020.

Stahl, W. L., and D. G. Baskin. 1984. Immunocytochemical localization of Na^+,K^+ Adenosine Triphosphatase in the rat retina. *J. Histochem. Cytochem.* 32:248–250.

Stirling, C. E., and A. Lee. 1980. [^{3}H]Ouabain autoradiography of frog retina. *J. Cell Biol.* 85:313–324.

Stirling, C. E., and P. V. Sarthy. 1985. Localization of the Na-K pump in turtle retina. *J. Neurocytol.* 14:33–47.

Ueno, S. H. Umar, H. J. Bambauer, and M. Ueck. 1984. Localization of ATPases in retinal receptor cells. *Ophthalmic Res.* 16:15–20.

Wolf, D. E. 1987. Overcoming random diffusion in polarized cells: corralling the drunken begger. *Bioessays.* 6:116–121.

Yazulla, S., and K. M. Studholme. 1987. Ultracytochemical distribution of ouabain-sensitive, K^+-dependent, p-nitrophenylphosphatase in the synaptic layers of goldfish retina. *J. Comp. Neurol.* 261:74–84.